

关于新型喷射-吸收式热变换器性能的分析

王子彪¹ 杨勃²

(1. 沈阳建筑大学 市政与环境工程学院 辽宁 沈阳 110168; 2. 天津天咨拓维建筑设计有限公司 天津 300070)

摘要: 针对传统热变换器系统温升低, 提出一种含有两个发生器的新型喷射-吸收式热变换器系统。与传统的热变换器相比, 该新型系统引入了一个低压发生器和喷射器: 来自蒸发器的高压冷剂蒸汽驱动喷射器, 低压发生器经喷射器的引射维持低压, 整个系统中溴化锂溶液低压降低了, 系统浓度差增大。对该新型热力模型进行分析, 结果显示: 系统热泵温升从传统热变换器的 17.6 °C 变为 25 °C, 提高了热品质。

关键词: 发生器 喷射器 吸收式热变换器 热力分析 热品质

中图分类号: TB616; TB65 文献标识码: A

DOI: 10.16146/j.cnki.rndlgc.2016.05.005

引言

余热的直接排放, 导致能源利用效率和经济效益降低, 间接增加石化能源的燃烧, 加重全球温室效应; 而高温废热的排放形成的热污染, 导致水生生物病变及死亡、加重城市热岛效应^[1~2]。热泵技术成为肩负清洁生产和节能降耗双重使命的重要技术之一^[3]。国内外许多学者主要从单级吸收式热变换器、两级和双效吸收式热变换器以及喷射-吸收式热变换器 3 个方面进行了大量研究^[4~11], 其中 Riv-era and Cerezo 就溴化锂升温型吸收式热泵加入添加剂正辛醇和乙基己醇进行了研究^[12], 结果显示: 相同条件下, 加入体积分数 400×10^{-6} 的乙基己醇将使吸收温度增加 5 °C, 相应的 COP 增加 40%; Kiyam Parham 等就双效升温型吸收式热泵吸收、蒸发器中浓溶液的 3 种不同接入点进行了对比分析^[13]。Alonso 等首个建立吸收-溶液分层式热变换器实验机构^[14], 以正庚烷/N,N-二甲基甲酰胺为工作混合物, 实验结果显示, 最大温升为 80 °C、效率在 0.3 到 0.4 之间。

本研究提出一种含有两个发生器的喷射-吸收式热变换器, 用于回收工业余热; 低压发生器的引入, 降低了系统中溴化锂溶液的最低压力, 增大了热泵温升。

1 模型原理

热泵温升和性能系数 COP 是热变换器的两个重要性能指标, 基于显著提高热变换器温升的目的, 新型双发生器喷射-吸收式热变换器可回收废热, 节能减排, 同进还可增大热变换器的温升。

新型双发生器喷射-吸收式热变换器系统模型如图 1 所示, 由于低压发生器的引入, 降低了溴化锂溶液的最低压力, 增大了该溶液的浓度, 根据溴化锂溶液物理特性, 浓度增大, 吸收压力不变, 吸收器出口温度增大, 热泵温升增大。

该模型流程如下:

(1) 溴化锂溶液的循环: 来自高压发生器的溴化锂稀溶液流入低压发生器, 被废热水加热产生低压冷剂蒸汽, 而溴化锂溶液浓度进一步提高, 成为高浓度溶液, 经泵加压流经溶液热交换器 I、II 后再进入吸收器。在吸收器中, 吸收来自蒸发器的高压冷剂蒸汽, 稀释为稀溶液, 并将热量释放给用户供水, 相应的稀溶液流入溶液热交换器 I, 再经过节流阀进入高压发生器, 在高压发生器中被废热水加热浓缩成中等浓度的溴化锂溶液, 依次经过溶液热交换器 II 和节流阀, 最终流入低压发生器, 完成溴化锂溶液的循环;

(2) 冷剂蒸汽的循环: 高压发生器中产生的冷剂蒸汽与喷射器出来的冷剂蒸汽混合后在冷凝器中被冷却水冷却成为冷剂液体, 经泵升压后进入蒸发器, 蒸发器内冷剂液体通过喷淋装置, 吸收了传热管

收稿日期: 2015-06-01; 修订日期: 2015-07-28

基金项目: 国家十二五科技支撑计划项目(2012BAJ26B02); 住房与城乡建设部项目(2013-K1-58); 沈阳建筑大学科研项目(2013141)

作者简介: 王子彪(1957-), 男, 沈阳建筑大学副教授。

通讯作者: 杨勃(1989-), 男, 天津天咨拓维建筑设计有限公司设计师。

内废热水的热量蒸发成高压冷剂蒸汽后,一部分进入吸收器,该部分冷剂蒸汽被溴化锂浓溶液所吸收,再经溶液循环带入高压发生器;另一部分高压冷剂蒸汽用于驱动喷射器,在喷射器中与来自低压发生器的冷剂蒸汽混合后喷出,最终与来自高压发生器的冷剂蒸汽混合,这样完成了冷剂蒸汽的循环。

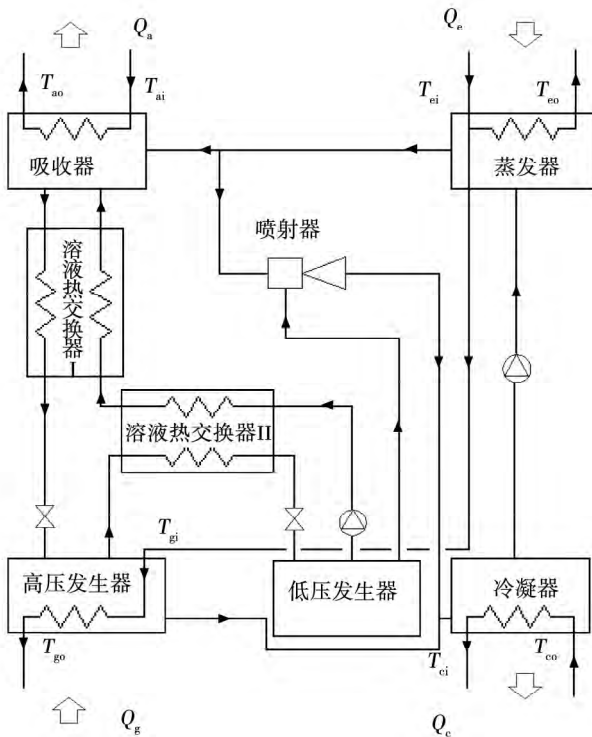


图 1 新型喷射吸收式热变换器流程图

Fig. 1 Flow chart for new type jet-absorption type heat converters

2 模型建立

2.1 数学模型

为了简化模型的求解,本研究对系统的热力计算模型以及仿真模型做了如下假设:

(1) 整个系统处于稳定流动状态,每个部件都满足能量平衡条件;(2) 各个换热设备内的工质均处于饱和状态;(3) 忽略流阻、热损失和压力损失,工质节流前后焓值相等;(4) 忽略各泵功率对系统的影响。

2.1.1 数学关联式

(1) LiBr - H₂O 溶液的焓^[15]:

$$h(w, t) = \sum_{i=0}^5 \sum_{j=0}^2 A_{ij} w^i t^j \quad (1)$$

LiBr - H₂O 溶液的露点,相应饱和水蒸气的温度^[15]:

$$t_{DP}(w, t) = \frac{5}{9} \left[\sum_{i=0}^5 \sum_{j=0}^2 B_{ij} w^i \left(32 + \frac{9}{5} t \right)^j - 32 \right] \quad (2)$$

式中: h —溴化锂溶液的焓, kJ/kg; t_{DP} —溴化锂溶液的露点温度, °C; t —溴化锂溶液的温度, °C; w —溴化锂溶液的浓度, %; 系数 A_{ij} , B_{ij} 的值见文献[15]。适用范围是: $0\% < w < 70\%$, $4.4\text{ °C} < t < 180\text{ °C}$ 。

(2) 饱和水的焓^[16]:

$$h_1 = -1295.6097 + 560.4922 \frac{T_1}{100} - 43.$$

$$7943 \left(\frac{T_1}{100} \right)^2 + 4.4794 \left(\frac{T_1}{100} \right)^3 + 1.2685 \times 10^{-2} P_1 - 2.$$

$$3458 \times 10^{-6} P_1 - 3.8715 \times 10^{-3} P_1 \left(\frac{T_1}{100} \right)^2 \quad (3)$$

式中: h_1 —饱和水焓, kJ/kg; T_1 —液态水的温度, K; P_1 —该状态下水的饱和压力, kPa。

(3) 饱和水蒸气的焓^[17]:

$$h_v = 1997.8546 + 0.9858 \times 10^{-2} P_v + 185.4761$$

$$\frac{T_v}{100} - 1.1942 \left(\frac{T_v}{100} \right)^2 + 0.3003 \left(\frac{T_v}{100} \right)^3 -$$

$$58.5024 P_v / \left(\frac{T_v}{100} \right)^3 - 256652.9031 P_v / \left(\frac{T_v}{100} \right)^{11} \quad (4)$$

式中: h_v —饱和水蒸气的焓值, kJ/kg; T_v —饱和水蒸气的温度, K; P_v —饱和水蒸气的压力, kPa。

(4) 水的饱和蒸汽压^[18]:

$$\ln P_v = 9.4865 + \frac{3892.7}{42.6776 - T_v} \quad (5)$$

式中: T_v —饱和水蒸气的温度, K; P_v —饱和水蒸汽的压力, MPa。

2.1.2 守恒关系式

(1) 质量守恒

$$\sum m_{in} = \sum m_{out} \quad (6)$$

$$\sum m_{in} \times w_{in} = \sum m_{out} \times w_{out} \quad (7)$$

式中: m_{in} —流进部件的质量流量, kg/s; m_{out} —流出部件的质量流量, kg/s; w_{in} —流进部件溴化锂溶液的浓度, %; w_{out} —流出部件溴化锂溶液的浓度, %。

(2) 能量守恒

$$\sum m_{out} \times h_{out} = \sum m_{in} \times h_{in} + Q \quad (8)$$

式中: h_{out} —流出部件的焓, kJ/kg; h_{in} —流进部件的焓, kJ/kg; Q —部件吸收的热量, kW。

(3) 传热关系式

$$Q = k \times \Delta T_m \times F \quad (9)$$

$$\Delta T_m = \frac{[(T_1 - T_2) - (T_3 - T_4)] / \ln [(T_1 - T_2) / (T_3 - T_4)]}{\quad} \quad (10)$$

式中: k —传热系数, $\text{kJ}/(\text{m}^2 \cdot \text{K})$; F —部件的换热面积, m^2 ; Q —部件吸收的热量, kW ; ΔT_m —对数平均温差, K ; T_1 —热流进口温度, K ; T_2 —热流出口温度, K ; T_3 —冷流进口温度, K ; T_4 —冷流出口温度, K 。

(4) 喷射器的动量守恒

$$G_P \omega_{P1} + G_H \omega_{H1} - (G_P + G_H) \omega_3 = p_3 f_3 + \int_{f_3}^{f_1} p df - (p_{P1} f_{P1} + p_{H1} f_{H1}) \quad (11)$$

式中: ω_{P1} —混合室入口截面上工作流体的速度, m/s ; ω_{H1} —混合室入口截面上引射流体的速度, m/s ; ω_3 —混合室入口截面上混合流体的速度, m/s ; p_{P1} —混合室入口截面上工作流体的静压力, N/m^2 ; p_{H1} —混合室入口截面上引射流体的静压力, N/m^2 ; p_3 —混合室出口截面上混合流体的静压力, N/m^2 ; f_{P1} —进入混合室时工作流体的截面积, m^2 ; f_{H1} —进入混合室时引射流体的截面积, m^2 ; f_3 —在混合室出口处混合流体的截面积, m^2 ; $\int_{f_3}^{f_1} p df$ —在 1—1 和 3—3 截面之间作用于混合室壁面上力的冲量积分。

喷射器的简图如图 2 所示。

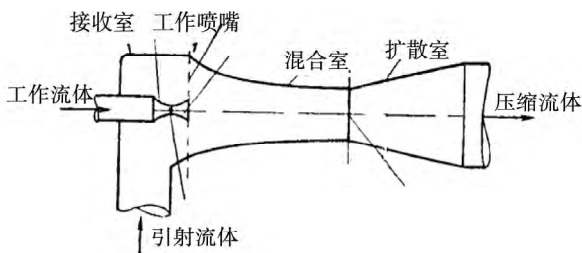


图 2 喷射器简图

Fig. 2 Sketch of the jet injector

(5) 喷射器的喷射系数 μ :

$$\mu = \frac{G_H}{G_P} \quad (12)$$

式中: G_H —引射流体的质量流量, kg/s ; G_P —工作流体的质量流量, kg/s 。

2.2 模型求解

由于上述模型是一个多元非线性方程组,且变量多、溴化锂溶液状态点的温度、浓度相互制约,本

研究采用 1stOpt 软件,选择简面体爬山算法进行求解。模型求解流程如图 3 所示,根据数学模型的边界条件及初设未知量,确定出各状态点参数,然后根据各部件的能量守恒方程和传热方程计算溴化锂溶液浓度 ξ 。通过观察是否结晶,以判断是否将对机组内各传热部件负荷及性能进行下一步计算。

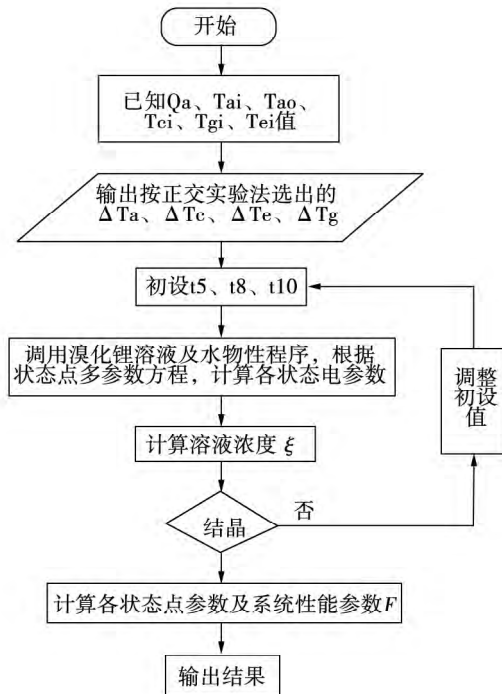


图 3 模型求解流程

Fig. 3 Flow chart for seeking solutions to the model

3 结果分析

3.1 喷射器分析

喷射器作为低压发生器的驱动装置,其喷射系数对系统起着至关重要的作用,喷射系数过低,意味着蒸发单位低压发生器的冷剂蒸汽所需要的工作蒸汽增大,即蒸发器的热负荷增大,系统的能效比 COP 降低,故喷射系数越大越对能效比有利。

3.1.1 冷却水出口温度对喷射系数的影响

冷却水出口温度对喷射器的工作性能至关重要,在不同出口温度下,冷却水出口温度与喷射系数的关系如图 4 所示,蒸发器废热水出口温度为 $49.2\text{ }^\circ\text{C}$ 。可知,随着冷却水出口温度降低,喷射系数增加很快。低压发生器压力为 0.8627 kPa ,当冷却水出口温度降低 11% (从 $18\text{ }^\circ\text{C}$ 变到 $16\text{ }^\circ\text{C}$) 的时

候 喷射系数则增加了约 34.3% (从 0.251 66 变为 0.337 97)。因此 降低冷却水出口温度可以改善喷射器工作效率。低压发生器压力的增加会导致最大喷射系数的增大。由图 4 可知,当低压发生器压力从 0.748 6 kPa 升高到 0.862 7 kPa 的时候,喷射系数增加很快。另外,在不同低压发生器压力下,冷却水出口温度对喷射系数影响程度是不一样的。在低压发生器压力为 0.748 6 kPa 的时候,冷却水出口温度同样从 18 °C 变为 16 °C,喷射系数从 0.213 54 变为 0.280 12,增加约小于 34%。

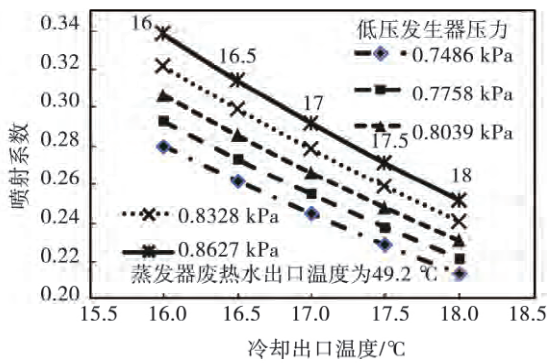


图 4 在不同低压发生器压力下,喷射系数与冷却水出口温度的关系

Fig. 4 Jet injection coefficient vs. the temperature at the outlet of the cooling water at various pressures inside the low pressure generator

3.1.2 低压发生器压力对喷射系数的影响

在不同低压发生器压力下,喷射系数与低压发生器压力的关系如图 5 所示。冷凝器冷却水出口温度为 16 °C,可知,喷射系数随着低压发生器压力的增加提升很快。在蒸发器废热出口温度为 49.2 °C 的时候,低压发生器压力从 0.748 4 kPa 增加到 0.862 7 kPa,喷射系数增加了 20% 以上 (从 0.280 12 到 0.337 97)。因此,增加低压发生器压力,可以增加喷射系数,提高喷射器工作的效率。

3.1.3 蒸发器废热出口温度对喷射系数的影响

如图 6 所示喷射系数随着蒸发器废热出口温度的增加而增加。并且在低压发生器压力为 0.862 7 kPa 的条件下,不同的冷凝器冷却水出口温度使得喷射系数随着蒸发器废热出口温度的增加而上升的趋势基本一致,且随着冷凝器冷却水出口温度的降低、蒸发器废热出口温度的增加,喷射系数迅速增大,当冷却水出口温度为 16 °C、蒸发器废热出口温度为 51.2 °C 时喷射系数最大为 0.368 26。

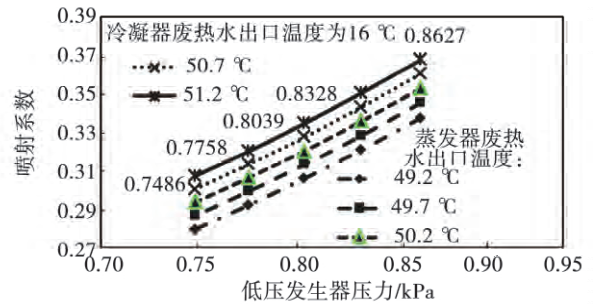


图 5 在不同蒸发器废热出口温度下,喷射系数与低压发生器压力的关系

Fig. 5 Jet injection coefficient vs. the pressure inside the low pressure generator at various waste heat temperature at the outlet of the evaporator

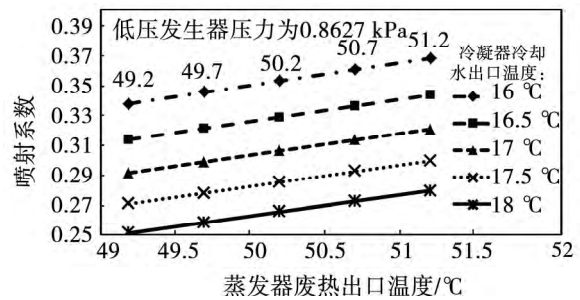


图 6 在不同冷却水出口温度下,喷射系数与蒸发器废热出口温度的关系

Fig. 6 Jet injection coefficient at the outlet of the cooling water vs. the waste heat temperature at the outlet of the evaporator at various temperatures

4 与传统热变换器的比较

用户供水温度提升,吸收压力不变,根据溴化锂溶液物理特性知,流出吸收器的稀溶液浓度增大,系统浓度差降低,如图 7 所示,当传统热变换器的供水温度从 66.6 °C 提升到 72.6 °C,相应的浓度差从 36.56% 降低到 1.57%;而新型热变换器供水温度从 66.6 °C 提升到 80 °C,相应的浓度差从 78.27% 变为 5.82%。可见,在 55 °C 的废水供热温度,传统热变换器的系统温升最大只有 17.6 °C,而新型热变换器的最大温升大于 25 °C。由于低压发生器的引入,大大增大了系统溴化锂浓溶液的浓度,使得在相同的用户供水温度下,新型热变换器的浓度差远远大于传统热变换器的;当用户供水温度为 66.6 °C 时,新型热变换器的浓度差比传统热变换器的要高 30% 多。另外,从图 7 可以看出,随着用户供水温度的增大,新型热变换器与传统热变换器的能效比

COP 均降低, 当废热供水温度从 66.6 °C 增大到 80 °C 时, 热变换器系统能效比 COP 从 0.243 1 降低到 0.188 1。而在相同的用户供水温度下, 新型热变换器的系统能效比 COP 要比传统热变换器的要低。

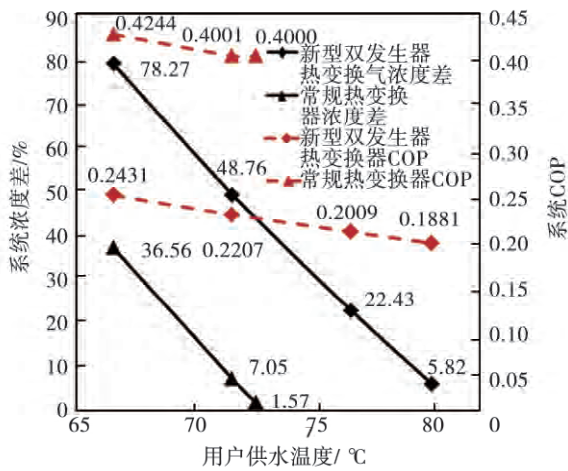


图 7 与传统吸收式热变换器的比较

Fig. 7 Comparison with the traditional absorption type heat converters

5 结 论

本研究提出的新型双发生器喷射 - 吸收式热变换器, 由于引入低压发生器, 系统最低压力降低, 系统浓度差增大, 当用户供水温度相同时, 新型热变换器的浓度差比传统的要高 30% 以上。最终导致热泵温升从传统热变换器的 17.6 °C 变为 25 °C, 提高了热品质。但是, 新型热变换器的能效比 COP 较传统热变换器的有所减小。

参考文献:

[1] 林 芃, 王如竹, 马 强. 低品位热能的远距离输送技术 [J]. 制冷学报, 2009, 30(5): 1 - 7.
LIN Peng, WANG Ru-zhu, MA Qiang. Low grade heat energy long distance transmission technology [J]. Journal of Refrigeration, 2009, 30(5): 1 - 7.

[2] 中国科学院学部. 我国工业节能现状调研和对策 [J]. 中国科学院院刊, 2010, 25(3): 307 - 308.
Academic Division under Chinese Academy of Sciences. Investigation of the status quo of the energy conservation in industry in China and its countermeasures [J]. Journal of Chinese Academy of Sciences, 2010, 25(3): 307 - 308.

[3] 史 琳, 王 文, 王 鑫 等. 新型喷射 - 吸收式变换器的研究 [J]. 工程热物理学报, 2001, 22(5): 543 - 546.
SHI Lin, WANG Wen, WANG Xin, et al. Study of a new type jet injection-absorption heat converter [J]. Journal of Engineering thermophysics, 2001, 22(5): 543 - 546.

[4] 郭培军, 隋 军, 金红光. 立式升温型溴化锂吸收式热泵的设

计与变工况研究 [J]. 工程热物理学报, 2012, 33(6): 907 - 912.

GUO Pei-Jun, SUI Jun, JIN Hong-Guang. Design and off-design condition study of a vertical temperature rise type LiBr absorption type heat pump [J]. Journal of Engineering thermophysics, 2012, 33(6): 907 - 912.

[5] 刘 辉, 于慧雪, 池 坤. 第二类吸收式热泵回收炼厂低温余热实例 [J]. 石化技术与应用, 2010, 28(2): 123 - 127.
LIU Hui, YU Hui-xue, CHI Kun. Example of a second category absorption type heat pump being used to recover the low temperature waste heat from an oil refinery [J]. Petrochemical Technology & Application, 2010, 28(2): 123 - 127.

[6] Kurem E, Horuz I. A comparison between ammonia-water and water-lithium bromide solutions in absorption heat transformers [J]. Int Commun Heat Mass Transf 2001; 28: 427 - 438.

[7] Horuz I, Kurt B. Absorption heat transformers and an industrial application [J]. Renew Energy 2010, 35: 2175 - 2181.

[8] 尹 娟, 史 琳, 朱明善 等. 二次提升型吸收式变换器热力学性能分析 [J]. 清华大学学报, 2000, 40(10): 88 - 91.
YIN Juan, SHI Lin, ZHU Ming-shan, et al. Thermal performance analysis of a secondary upgradation type heat converter [J]. Journal of Tsinghua University, 2000, 40(10): 88 - 91.

[9] 马学虎, 李 达, 郝兆龙 等. 高温双再生器型吸收式热变换器热力循环分析 [J]. 大连理工大学学报, 2012, 52(6): 794 - 798.
MA Xue-hu, LI Da, HAO Zhao-long, et al. Analysis of the thermodynamic cycle of a high temperature dual regenerator type absorption heat transformer [J]. Journal of Dalian University of Science and Technology, 2012, 52(6): 794 - 798.

[10] Alonso D, Cachot T, Hornut JM. Experimental study of an innovative absorption heat transformer using partially miscible working mixtures [J]. Int J Therm Sci 2003; 42: 631 - 638.

[11] 苏庆泉, 孙 鹏, 罗春欢 等. 一种新型第二类吸收式热泵的原理及性能分析 [J]. 太阳能学报, 2012, 33(2): 297 - 311.
SU Qing-quan, SUN Peng, LUO Chun-huan, et al. Principles and performance analysis of a new type second category absorption type heat pump [J]. Acta Energetica Solaris Sinica, 2012, 33(2): 297 - 311.

[12] Rivera W, Cerezo J. Experimental study of the use of additives in the performance of a single-stage heat transformer operating with water-lithium bromide [J]. Int J Energy Res 2005; 29: 121 - 130.

[13] Kiyani Parham, Mehrdad Khamooshi. Absorption heat transformers-A comprehensive review [J]. Renewable and Sustainable Energy Reviews 2014, 22(5): 430 - 452.

[14] Alonso D, Cachot T, Hornut JM. Experimental study of an innovative absorption heat transformer using partially miscible working mixtures [J]. Int J Therm.

[15] M. R Patterson and H. Perez-Blanco. Numerical fits of the properties of the lithium-bromide water solutions [J]. ASHRAE Trans, 1988, 94(2): 2059 - 2077.

[16] 贾明生. 溴化锂水溶液的 几个主要物性参数计算方程 [J]. 湛江海洋大学学报, 2002, 22(3): 52 - 58.
JIA Ming-sheng. Equation for calculating several parameters of Li-Br-H₂O water solution in physical property [J]. Journal of Zhanjiang Oceanology University, 2002, 22(3): 52 - 58.

[17] Irvine T F. Steam and gas tables with computer equations [M]. Uemura T, New York: Academic Press, 1984.

[18] Sun Dawen. Thermodynamic design data and optimum design maps for absorption refrigeration systems [J]. Applied Thermal Engineering, 1997, 17(3): 211 - 221.

(刘 瑶 编辑)

performance of a stepped heat exchange ORC system. **Key words:** heat source flow division ,stepped heat exchange ,organic Rankine cycle ,critical temperature ,nearing critical point

水平管外降膜厚度分布规律的数值模拟研究 = **Numerical Simulation Study of the Law Governing the Distribution of the Falling-film Thickness Outside a Horizontal Tube** [刊 汉] CAI Zhen ,ZHOU Yi-hui ,BI Ming-shu ,REN Jing-jie (College of Chemical Machinery ,Dalian University of Science and Technology ,Dalian ,China , Post Code: 116024) //Journal of Engineering for Thermal Energy & Power. -2016 31(5) . -22 ~28

The law governing the distribution of the liquid film thickness exercises an important influence on the falling film evaporation process outside a horizontal tube. A CFD model for the falling film flow outside a horizontal tube was established and through simulating the liquid film thickness at various inlet speeds and different sizes of the diameter of the tube ,the factors influencing the liquid film thickness outside the tube in the cold state and the law governing its distribution along the circumferential angle were studied. The simulation results show that for a constant diameter of the tube ,the liquid film thickness will increase with an increase of the inlet speed. When the inlet speed is constant ,the liquid film thickness outside the tube will be relatively big in the zone at the top of the tube and arrive at its minimum around a place at a circumferential angle of 105 degrees. Moreover ,the liquid film thickness will gradually decrease with an increase of the tube diameter. When the inlet speed decreases to a certain extent ,the “dry-up” phenomenon will appear on the tube wall. **Key words:** falling film flow outside a horizontal tube ,liquid film thickness ,inlet speed ,tube diameter ,circumferential angle

关于新型喷射-吸收式热变换器性能的分析 = **Analysis of the Performance of a Novel Jet-absorption Type Heat Converter** [刊 汉] WANG Zi-biao ,YANG Bo (College of Municipal and Environmental Engineering ,Shenyang Architectural University ,Shenyang ,China ,Post Code: 110168) //Journal of Engineering for Thermal Energy & Power. -2016 31(5) . -29 ~33

In the light of the low temperature rise in the traditional heat converter systems ,proposed was a new type jet-absorption heat converter system with two generators. Compared with the traditional heat converters ,a low pressure generator and jet ejector was introduced into the system in question: the jet ejector was driven by the high-pressure refrigerant vapor from the evaporator and the low pressure in the low pressure generator was maintained by the jet ejector , thus leading to a drop of the pressure of the lithium bromide solution in the whole system and a rise of the concentration difference in the system. An analysis of the thermal model for the system under discussion shows that the

temperature rise of the heat pump in the system increases from the temperature rise of 17.6 °C in the traditional heat convertor to 25 °C ,therefore ,enhancing the heat quality ,**Key words:** generator ,jet ejector ,absorption-type heat convertor ,thermodynamic analysis ,heat quality

强化蒸发管形成碳酸钙污垢的特性研究 = Study of the CaCO₃ Foul Characteristics of an Intensified Evaporation Tube [刊 ,汉] WANG Yan-kun ,ZHANG Hua ,YOU Xiao-kuan ,SHENG Jian (Refrigeration Technology Research Institute ,Shanghai University of Science and Technology ,Shanghai ,China ,Post Code: 200093) //Journal of Engineering for Thermal Energy & Power. -2016 ,31(5) . - 34 ~ 39

With an intensified evaporation tube serving as the object of study ,investigated was the law governing the fouling of CaCl₂-Na₂CO₃ solution on the surface of a bare tube ,a plane and straight obliquely-finned tube and a sawtooth-shaped obliquely-finned tube. A constant initial foul formation ion concentration method was adopted ,i. e. no foul-formation ion was added in the process of foul formation during the test. For several types of heat exchange tube and bare tube ,the foul resistant effectiveness was tested respectively at various temperatures and flow speeds. The test results show that the amount of foul formed on No. 1 plane and straight finned tube is largest ,far larger than that formed on the bare tube. The amount of foul formed on No. 2 straight finned tube is smallest. The fouling resistance of the sawtooth-shaped finned tube is close to that of the bare tube ,thus the types of their foul being also similar.

Key words: intensified heat transfer ,CaCO₃ foul ,intensified evaporation tube

超临界 CO₂ 发电循环特性分析 = Analysis of the Power Generation Cycle Characteristics of Supercritical Carbon Dioxide [刊 ,汉] LIAO Ji-xiang ,ZHENG Qun ,ZHANG Hai(College of Power and Energy Engineering , Harbin Engineering University ,Harbin ,China ,Post Code: 150000) ,LIU Xing-ye(College of Architectural Engineering ,Heilongjiang University of Science and Technology ,Harbin ,China ,Post Code: 150022) //Journal of Engineering for Thermal Energy & Power. -2016 ,31(5) . - 40 ~ 46

Five types of supercritical carbon dioxide power generation cycle were analyzed ,namely ,simple recuperative cycle , recompression cycle ,partial cooling cycle ,pre-compression cycle and subsection expansion cycle. Under the same operating parameters ,the thermal efficiencies of the cyclic systems above mentioned were analyzed and compared. It has been found that both efficiencies of the recompression cycle and the partial cooling one are the highest ,approaching to 45% . However ,the highest efficiency of the partial cooling cycle can result only at a high pressure ratio while the efficiency of the cycle in question at a low pressure ratio has no obvious cutting edge when compared with